Direct observation of the pH-dependent equilibrium between L-like and M intermediates of photoactive yellow protein

Yasushi Imamoto*, Miki Harigai, Mikio Kataoka

Graduate School of Materials Science, Nara Institute of Science and Technology, Ikoma, Nara 630-0192, Japan

Received 3 August 2004; revised 22 September 2004; accepted 22 September 2004

Available online 7 October 2004

Edited by Gerrit van Meer

Abstract **Equilibrium between the photoproducts of photoactive yellow protein (PYP), present in a millisecond time scale, was studied. The near-UV intermediate of PYP (PYP_M) was red-shifted by alkalization due to the deprotonation of the chromophore ($pK_a = 10.2$). In addition, a small amount of red-shifted intermediate coexisted with PYP_M. Its spectral shape in the visible region agreed with that of PYP_L, the precursor of PYP_M. The fraction of PYP_L-like product was maximal at pH 10. It decays with a rate constant identical to that of PYP_M. These results indicate that PYP_L-like product is in pH-dependent equilibrium with PYP_M and deprotonated PYP_M.**

Keywords: Photoreaction cycle; Intermediate; PAS domain; Conformational change; pH titration

1. Introduction

Photoactive yellow protein (PYP) is a water-soluble photoreceptor protein found in the purple phototropic bacterium, *Halorhodospira halophila* [1]. The phenolic oxygen of its *p*-coumaric acid chromophore in dark state is deprotonated, and forms hydrogen-bonds with the hydroxy groups of Tyr42 and Glu46 [2]. The absorption maximum of PYP is regulated by these amino acid residues as shown by 10–14 nm red-shifts upon mutation of these residues [3–5].

On photon absorption by the chromophore, it is isomerized from the *trans* to *cis* form. PYP subsequently undergoes a photoreaction cycle in which several intermediates are formed [6–10]. In the last stage of the photocycle, a blue-shifted intermediate (called PYP_M, pB, or I_2) is formed (Fig. 1). PYP_M has a lifetime of ~100 ms and is considered to be the signaling state. Accumulated evidence has shown several reactions at the amino acid level that accompany the formation of PYP_M.

The chromophore of PYP_L (a precursor of PYP_M) remains deprotonated and hydrogen-bonded with Tyr42 and Glu46 [11–14]. In this stage, difference in protein structure from the dark state is small [11,12]. On the decay of PYP_L, a proton at Glu46 is transferred to the chromophore [15]. As a result, the chromophore becomes electronically neutral and Glu46 negatively charged (pB′ state). This rearrangement of the hydrogen-bonding network around the chromophore induces a global conformational change of the protein moiety [11,12,16,17] (PYP_M or pB). It then reverts to the dark state via putative pB^{deprot} [18]. Recently, the photocycle of PYP was analyzed by considering equilibria between the intermediates [18,19]. The equilibria between pR (PYP_L) and pB′, and between pB and pB^{deprot} were incorporated, but the transition from pB′ to pB was considered to be irreversible. This reaction model reproduced the kinetics (time-resolved absorbance change) well, but the shapes of the negative absorption band of the transient difference spectra in the subsecond time scale were inconsistent with the dark-state spectrum at the long-wavelength tail (460–500 nm) [18]. In this wavelength region, there is no spectral overlap between PYP_M and PYP because PYP_M is a blue-shifted intermediate. Therefore, the disagreement between spectra strongly suggests the coexistence of a red-shifted intermediate.

Here, we studied the photocycle of PYP at alkaline pH, at which a significant amount of red-shifted intermediate with an absorption spectrum that agrees with that of PYP_L is in equilibrium with PYP_M.

2. Materials and methods

2.1. Sample preparation

PYP and its E46Q mutant were heterologously overexpressed by *Escherichia coli* and reconstituted by adding *p*-coumaric anhydride [3,20]. Because the thioester bond of the chromophore is readily hydrolyzed at high pH (pH > 10 in the presence of guanidinium hydrochloride (Gdn-HCl), pH > 11 without Gdn-HCl), PYP stock solution (17 mg ml^{-1}) or lyophilized powder was suspended in the buffer at alkaline pH just before the experiments.

2.2. UV–visible spectroscopy

UV–visible spectra were measured by a multichannel fiber optics system (S2000, Ocean Optics, USA). A deuterium lamp (Hamamatsu Photonics, Japan) was used as the monitoring light source. Temperature of the sample was kept constant by circulating temperature-controlled water. For steady-state measurement, the sample was irradiated with a yellow light (>430 nm) obtained using a glass optical filter (Y45, Asahi Techno Glass, Japan) and a cold light source (HL150, Hoya-Schott, Japan). For the time-resolved measurements, the sample was excited with a yellow flash (>410 nm) obtained using a glass optical filter (Y43, Asahi Techno Glass, Japan) and a short arc xenon flash lamp (SA200, Eagle, Japan), triggered by a delay pulse generator (DG535, Stanford Research Systems, USA). The spectral measurements were completed within 2 min.

* Corresponding author. Fax: +81-743-72-6109.
E-mail address: imamoto@ms.naist.jp (Y. Imamoto).

Abbreviations: PYP, photoactive yellow protein from *Halorhodospira halophila*; Gdn-HCl, guanidinium hydrochloride

0014-5793/$22.00
doi:10.1016/j.febslet.2004.09.065

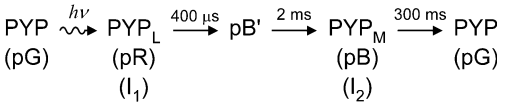

Fig. 1. Photocycle of PYP over microsecond time scale.

2.3. pH titration of denatured PYP and PYP_M

PYP sample (pH 2.7, 20 °C), in which about 70% of PYP is converted to the colorless form due to protonation of the chromophore, was irradiated with >450 nm light. As PYP_M is extremely stable at pH 2.7, irradiation of the equilibrium mixture of PYP and its colorless form accumulates PYP_M completely. After confirming no absorbance at 446 nm, two volumes of 6 M Gdn-HCl were added to the sample to denature PYP_M. $E46Q_M$ was similarly denatured after irradiating E46Q at pH 3.6 at 4 °C. Dark-state PYP and E46Q were denatured by adding Gdn-HCl in the dark.

For pH titration, a small volume of 1–10 N NaOH was added to the sample. The absorbance increase at difference maximum (400 or 411 nm) was plotted against pH, and the pK_a and Hill coefficients were estimated by fitting with the following equation.

$$\mathrm{Abs} = a + \frac{b}{1 + 10^{n(\mathrm{p}K_a - \mathrm{pH})}} \quad (1)$$

where Abs is absorbance at difference maximum, a and $a+b$ are absorbance in the completely acidic and alkaline forms, respectively, and n is an apparent Hill coefficient.

2.4. Equilibrium between PYP_L, PYP_M and PYP_M^{410}

Absorption spectra of PYP sample at various pH values under illumination were obtained by steady-state measurement. To estimate the fractions of PYP_L, PYP_M and its deprotonated form (PYP_M^{410}) at each pH, the difference absorption spectrum between the dark state and the photo-steady-state mixture was decomposed into dark-state spectrum, difference spectrum between PYP_L and PYP (PYP_L/PYP spectrum), and the sum spectrum of PYP_M and PYP_M^{410} (see Section 3). PYP_M was dominant at acidic pH, whereas the equilibrium shifted towards PYP_L and PYP_M^{410} after alkalization. Therefore, the equilibrium is described as follows:

$$\mathrm{PYP_L} \underset{-n_1\mathrm{H^+}}{\overset{+n_1\mathrm{H^+}}{\rightleftarrows}} \mathrm{PYP_M} \underset{+n_2\mathrm{H^+}}{\overset{-n_2\mathrm{H^+}}{\rightleftarrows}} \mathrm{PYP_M^{410}} \quad (2)$$

The dissociation constants for the left- and right-hand equilibria (K_1 and K_2, respectively) are expressed as

$$K_1^{n_1} = \frac{[\mathrm{PYP_L}][\mathrm{H^+}]^{n_1}}{[\mathrm{PYP_M}]} \quad (3)$$

$$K_2^{n_2} = \frac{[\mathrm{PYP_M^{410}}][\mathrm{H^+}]^{n_2}}{[\mathrm{PYP_M}]} \quad (4)$$

Assuming that no intermediate states are present between PYP_L and PYP_M, and between PYP_M and PYP_M^{410}, the fractions of PYP_L, PYP_M and PYP_M^{410} are given by

$$[\mathrm{PYP_L}] = \frac{1}{1 + 10^{-n_1(\mathrm{pH}-\mathrm{p}K_1)} + 10^{-n_1(\mathrm{pH}-\mathrm{p}K_1)+n_2(\mathrm{pH}-\mathrm{p}K_2)}} \quad (5)$$

$$[\mathrm{PYP_M}] = \frac{1}{1 + 10^{n_1(\mathrm{pH}-\mathrm{p}K_1)} + 10^{n_2(\mathrm{pH}-\mathrm{p}K_2)}} \quad (6)$$

$$[\mathrm{PYP_M^{410}}] = \frac{1}{1 + 10^{n_1(\mathrm{pH}-\mathrm{p}K_1)-n_2(\mathrm{pH}-\mathrm{p}K_2)} + 10^{-n_2(\mathrm{pH}-\mathrm{p}K_2)}} \quad (7)$$

The fractions of PYP_L, PYP_M and PYP_M^{410} were plotted against pH, and fitted by these functions using a global fit program (Igor Pro. ver 3.14, WaveMetrix, USA).

2.5. FTIR spectroscopy

FTIR spectra were measured using a BioRad FTS-6000 Fourier transform infrared spectrophotometer. Temperature of the sample was maintained by an Oxford Optistat DN optical cryostat. The sample cell was composed of two CaF_2 windows (18 mm diameter) and a Capton film spacer (7.2 mm thickness, Toray-Dupont, Japan), in which 160 mg ml^{-1} sample was placed. Sample was irradiated with a 436 nm light obtained using an optical interference filter (Edmund Scientific, USA) and a cold light source (HL150, Hoya-Schott, Japan).

3. Results and discussion

3.1. Equilibrium between PYP_M and PYP_L

The typical photoreaction of PYP at alkaline pH is shown in Fig. 2A. PYP at pH 10.0 was excited by a yellow flash (>410 nm) and the subsequent spectral change over a millisecond time scale was recorded (Fig. 2A). Just after excitation, PYP is converted to PYP_M, as shown by the absorbance decrease at 446 nm, with a concomitant increase at 352 nm. At pH 10.0, a clear absorbance increase at 485–510 nm was also observed. As it has not been observed at acidic pH, it is not likely to be a sub-absorption band of PYP_M. Thus, the small absorbance increase indicates coexistence of a small amount of a red-shifted intermediate. Since the spectral shape of this red-shifted intermediate agrees with that of PYP_L (see below), it is tentatively identified as PYP_L. PYP_L and PYP_M decayed with clear isosbestic points at 483 and 383 nm. The absorbance changes at 446, 352, and 491 nm are plotted against time after excitation, and independently fitted with single-exponential curves (Fig. 2B). As the rate constants at 352, 446, and 491 nm agreed with each other (3.57, 3.61, and 3.62 s^{-1}, respectively), PYP_L and PYP_M decay simultaneously in this time scale. However, transient spectroscopy in microsecond time scale demonstrated that the apparent decay rate constant of PYP_L is $\sim 10^4$ s^{-1} at pH 7–10 [4]. These findings indicate that PYP_L decays as a double-exponential function, having rate constants of ~ 3 s^{-1} and $\sim 10^4$ s^{-1}. If PYP_L decays irreversibly, the presence of a slow phase in a millisecond time scale cannot be explained. Therefore, the agreement between the decay rate constants of PYP_L and PYP_M indicates that PYP_L is in equilibrium with PYP_M, as shown by Eq. (2). Since the absorbance increase for persistence of PYP_L was small at neutral pH, it has been overlooked. Thermal equilibrium between PYP_L and PYP_M (I_1 and I_2) has been suggested by the analysis of kinetics of E46Q [19].

3.2. Calculation of the absorption spectrum of PYP_M and its deprotonated form

Absorption spectrum of PYP_M is red-shifted at alkaline pH [21] (in this paper, PYP_M in the red-shifted form is tentatively called PYP_M^{410}). To analyze in detail the equilibrium between PYP_L, PYP_M and PYP_M^{410}, the absorption spectra of photo-steady-state mixtures at pH 8.0–11.5 were measured. Typical data (pH 10.0) are shown in Fig. 3.

Absorption spectra were measured in the dark (curve 1) and under continuous illumination with >430 nm light (curve 2). Absorbance at 446 nm was decreased, whereas at 352 and 491 nm was increased by illumination. As shown in the inset of Fig. 3A, the difference spectrum between photo-steady-state and dark state (light/dark spectrum; curve 3 in Fig. 3B) agrees with the transient difference spectrum just after excitation (Fig. 2A). Steady-state difference spectrum and transient difference spectrum were measured at several pH values, but agreed with each other. This indicates that the shift in equilibrium from the photo-reversal of intermediate(s) using continuous yellow light is negligible. Steady-state difference spectra were used in the analysis below, because steady-state measurement is superior to transient measurement in terms of signal-to-noise ratio.

The absorption spectrum of PYP intermediates has recently been studied in detail [18]. However, it was found that the measured ground state spectrum was not suitable for

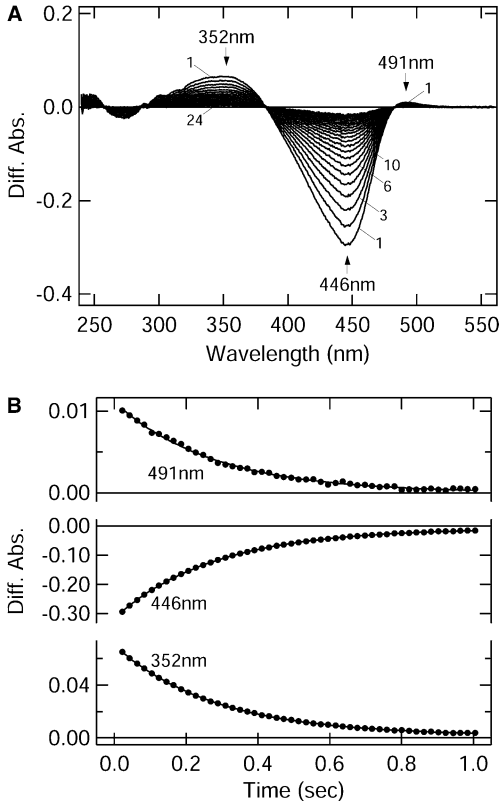

Fig. 2. Spectral change of PYP after excitation at alkaline pH. (A) PYP (10 mM CAPS, 200 mM NaCl, pH 10.0) was excited by a >410 nm flash and transient difference spectra before and after excitations were recorded at 20 °C (40 ms interval). (B) Absorbance changes at 352 (decay of PYP_M), 446 (recovery of PYP), and 491 nm (decay of PYP_L) were plotted against the time after excitation (20 ms interval). They were fitted by single-exponential curves, and rate constants were estimated to be 3.57, 3.61, and 3.62 s^{-1}, respectively.

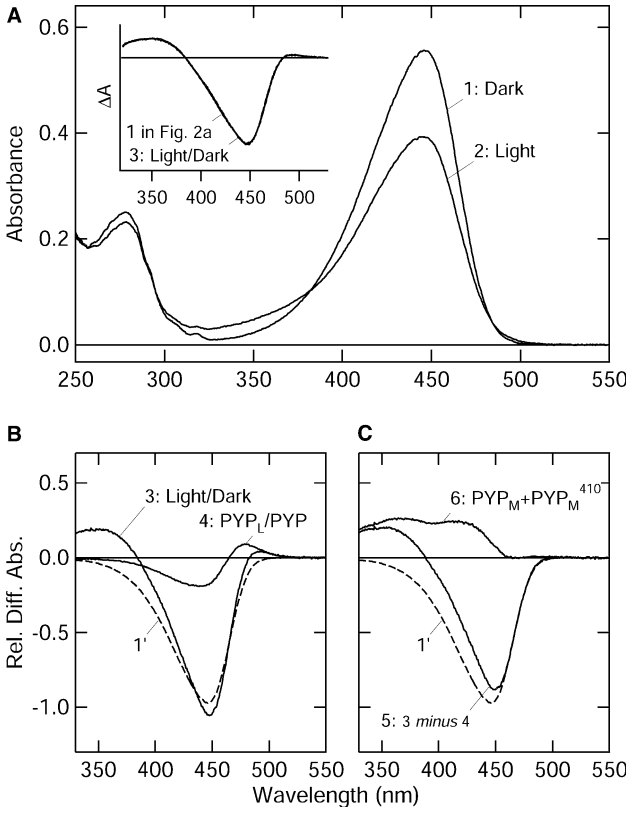

Fig. 3. Calculation of the absorption spectrum of a mixture of PYP_M and PYP_M^{410}. (A) Absorption spectra of PYP (20 mM glycine, 200 mM NaCl, pH 10.0) were measured in the dark (curve 1) and under continuous illumination with a >430 nm light (curve 2) at 20 °C. Inset: Comparison of the light/dark spectrum (curve 3; curve 2 minus curve 1) with the transient spectrum after flash excitation (reproduced from curve 1 in Fig. 2A). (B) Curve 1′ is the mirror image of curve 1 in (A). Curve 3 is the same as that in the inset of (A). PYP_L/PYP spectrum (curve 4) was reproduced from [22]. Curves 1′ and 3 were normalized by the (difference) absorbance at 465 nm (isosbestic point of PYP_L/PYP spectrum), and curves 3 and 4 were normalized by the absorbance at >500 nm. (C) Curve 4 was subtracted from curve 3 to remove the contribution of PYP_L (curve 5). Note that the shape of the spectral tail at >460 nm was identical to that of PYP (curve 1′). The sum of absorption spectra of PYP_M and PYP_M^{410} (curve 6) was calculated by subtracting curve 1′ from curve 5.

analyzing the transient difference spectra. Instead, the calculated spectrum (combination of skewed Gaussian), in which the spectral tail of the long-wavelength side (460–500 nm) is sharpened, was used. The mirror image of the dark-state spectrum (curve 1′) is compared with the light/dark spectrum (Fig. 3B). Spectral disagreement in the long-wavelength side is also seen in the present experiment. We found that this deviation agrees well with the PYP_L/PYP spectrum below.

The light/dark spectrum was decomposed into PYP_L, PYP_M and PYP_M^{410} spectra as follows. As the extinction coefficients of PYP and PYP_L at 465 nm are equal [22], absorbance decrease at 465 nm in light/dark spectrum is ascribed to the conversion from PYP to PYP_M and/or PYP_M^{410}. Thus, the amplitude of PYP spectrum (curve 1′), normalized by the absorbance at 465 nm in the light/dark spectrum, represents the amount of PYP converted to PYP_M and/or PYP_M^{410}. To eliminate the contribution of PYP_L from the light/dark spectrum, PYP_L/PYP spectrum (curve 4) was subtracted from light/dark spectrum so that the absorbance at >500 nm is cancelled by eye (curve 5 in Fig. 3C). The shape of the resultant spectrum at >460 nm agreed with that of PYP spectrum (Fig. 3C), confirming that the absorption spectrum of the red-shifted intermediate is indistinguishable from that of PYP_L. Absorption spectrum of the mixture of PYP_M and PYP_M^{410} at this pH was obtained by subtracting curve 1′ from curve 5. These sets of measurements and calculations were carried out for pH 8.0–11.5.

The amount of PYP converted to PYP_M and/or PYP_M^{410} is equal to the amplitude of curve 1′ at each pH, but it cannot be compared directly with that at different pH values because the absorption spectrum of PYP is slightly blue-shifted and reduced in height at alkaline pH [23] (2 nm blue-shift and 10% reduction at pH 11 under our experimental conditions). As the isosbestic point for this spectral change was 414 nm (data not shown), the amount of PYP converted to PYP_M and/or PYP_M^{410} was estimated by absorbance at 414 nm (curve 1′).

3.3. pH titration of native and denatured PYP_M

In addition to PYP_L, PYP_M and PYP_M^{410}, pB′, which is observed between PYP_L and PYP_M in transient spectroscopy [18], is possibly formed in the photo-steady-state. As the absorption spectrum of pB′ is located between PYP_M and

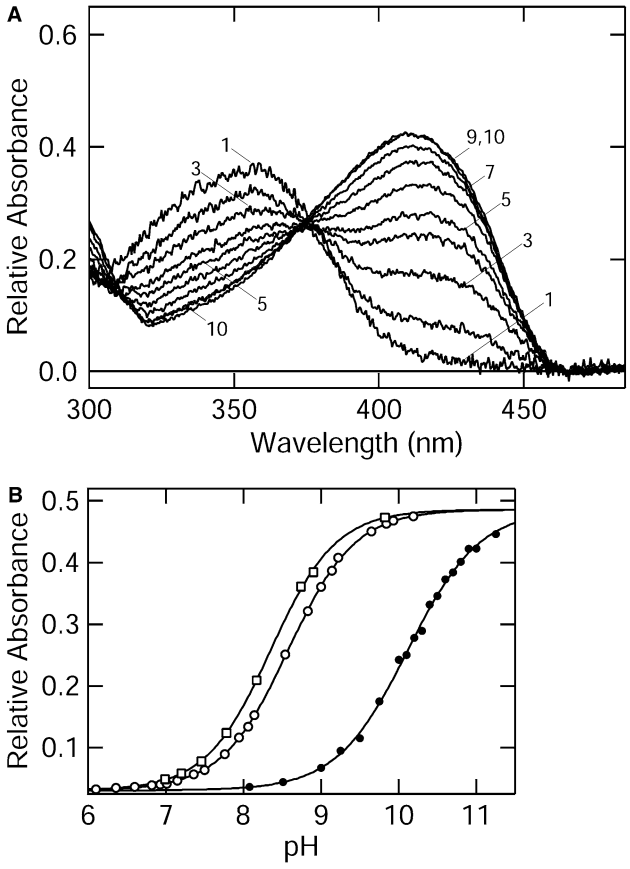

Fig. 4. pH titration of PYP_M. (A) Absorption spectra of the mixture of PYP_M and PYP_M^{410} at pH 8.1, 9.3, 9.8, 10.0, 10.2, 10.4, 10.6, 10.8, 10.9, and 11.0 (curves 1–10, respectively) were calculated according to the methods in Fig. 3. They are normalized by the amplitude of the dark state spectrum. Absorption maximum of PYP_M in protonated and deprotonated forms are 357 and 411 nm, respectively. (B) Relative absorbance at 411 nm in (a) was plotted against pH (closed circles). For comparison, absorbance at 400 nm of PYP (open squares) and PYP_M (open circles) denatured in the presence of 2 M Gdn-HCl was plotted against pH.

PYP_M^{410}, it should be detectable by UV–visible spectroscopy. The calculated spectra of the mixtures of PYP_M and PYP_M^{410} at various pH values are shown in Fig. 4A. Absorption spectrum of PYP_M is red-shifted at pH > 9 and finally the absorption maximum is shifted to 411 nm. As the isosbestic point was observed at 376 nm in this conversion, the formation of pB′ is negligible at alkaline pH.

Absorbance at 411 nm was plotted against pH and fitted by Eq. (1) (Fig. 4B). Apparent pK_a and Hill coefficient were estimated to be 10.1 and 0.9, respectively. In control experiments, PYP and PYP_M were denatured by 4 M Gdn-HCl, and pH titration experiments were carried out by addition of NaOH (Fig. 4B). This experiment gave pK_a and Hill coefficients of free *p*-coumaric acid thioester in *trans* and *cis* forms. The results demonstrate that for the *cis* form, absorption maximum was shifted from 341 to 399 nm by alkalization (Table 1). The latter was 12 nm shorter than that of PYP_M^{410}. The apparent pK_a and Hill coefficient were 8.6 and 1.0, respectively (Table 1). For the *trans* form, absorption maximum was shifted from 339 to 397 nm with a pK_a of 8.4 and Hill coefficient of 1.0 (Table 1). The absorption maxima as well as pK_a of native PYP_M were different from those of denatured PYP or PYP_M. To confirm whether these differences are due to the native structure of the protein moiety, the same titration experiments were carried out using denatured E46Q and $E46Q_M$. Absorption maxima (339 → 396 nm for *trans* form; 340 → 398 for *cis* form), pK_a (8.5 for *trans* and *cis* forms), and Hill coefficients (1.1 for *trans* form, 1.0 for *cis* form) were comparable to those of denatured PYP and PYP_M, while the absorption maximum and pK_a of dark state E46Q is significantly different from dark state PYP (Table 1). Therefore, the pK_a and absorption maximum of PYP_M are regulated by the native structure of the protein moiety, indicating that the chromophore of PYP_M is not completely exposed to solvent.

3.4. pH-dependent equilibrium between PYP_L, PYP_M and PYP_M^{410}

The amount of PYP_L in the photo-steady-state mixture is proportional to the amplitude of the PYP_L/PYP spectrum subtracted from the light/dark spectrum (Fig. 3, curve 4). The extinction coefficient of PYP_L at 475 nm is 1.9 times larger than that of PYP [10]. Using this value, the amount of PYP converted to PYP_L was calculated. Ratios of PYP_M and PYP_M^{410} were estimated from Fig. 4. The amounts of PYP_M, PYP_M^{410} and PYP_L in the photo-steady-state mixture were plotted against pH to quantitatively analyze the pH-dependent equilibrium between PYP_M, PYP_M^{410} and PYP_L, (Fig. 5). They were fitted with Eqs. (5)–(7) using a global fit program (Fig. 5), which gave values of 10.4 and 10.2 for pK_1 and pK_2, and 0.4 and 0.9 for n_1 and n_2, respectively. As apparent Hill coefficients for PYP_M, denatured *trans* and *cis* forms were ~1 (Table 1),

Table 1
Absorption maxima, pK_a and Hill coefficients

	PYP		PYP_M		E46Q		$E46Q_M$
	N[a]	D[b]	N	D	N	D	D
λ_{max}[c] (nm)							
Protonated	350	339	357	341	353	339	340
Deprotonated	446	397	411	399	460	396	398
pK_a	2.5[d]	8.4	10.2	8.6	5.3[e]	8.5	8.5
Hill coefficient	2.0[d]	1.0	0.9	1.0	0.9[f]	1.1	1.0

[a] Native state.
[b] Denatured state.
[c] Absorption maximum.
[d] Value from [25].
[e] Value from [3].
[f] Estimated from the data in [3].

their spectral red-shift after alkalization is explained by deprotonation of the chromophore. However, n_1 was estimated to be 0.4, suggesting that the reverse reaction from PYP_M to PYP_L driven by alkalization is not explained solely by deprotonation of the chromophore. It is consistent with the fact that large protein conformational changes take place on conversion from PYP_L to PYP_M.

3.5. Structure of PYP_M^{410} and PYP_L

A detailed study of PYP photocycle at alkaline pH clearly demonstrated the formation of a red-shifted intermediate over a millisecond time scale. As its absorption spectrum agrees well with PYP_L and it decays concomitant with PYP_M, it is reasonable to speculate that PYP_L is in equilibrium with PYP_M. The agreement of absorption spectra suggests that the chromophore structures and chromophore/protein interactions of PYP_L over the microsecond and millisecond time scales are comparable.

To obtain information about the protein structure of PYP_M^{410} and PYP_L, difference FTIR spectra between dark state and photo-steady-state were recorded at pH 9–11 (Fig. 6). The 1163 cm^{-1} mode for dark state is the marker of deprotonation of the chromophore [24]. It disappeared for photo-steady-state at pH 9.0, indicating that the chromophore of PYP_M is protonated. However, its complementary mode at 1170 cm^{-1} was observed for photo-steady-state at pH 10–11, which is consistent with the formation of PYP_M^{410} and PYP_L. The positive band at 1732 cm^{-1}, which is assigned to protonated Glu46, is observed for PYP_L trapped at 193 K [13] or a microsecond time scale [12]. However, the significant shift of 1736 cm^{-1} mode was not detectable from alkalization. The amount of PYP_L is too small to measure a high quality FTIR spectrum, but the possibility that the protein structure of PYP_L in the millisecond time scale is different from that in the microsecond time scale cannot be excluded.

PYP_M^{410} is formed at high pH and seems to be an alkaline-denatured form. However, FTIR spectroscopy demonstrated that the absorbance change in amide I mode of PYP_M^{410}/PYP spectrum was comparable to that of PYP_M/PYP spectrum, indicating that the protein structures of PYP_M^{410} and PYP_M are comparable. Thus, the protein conformation of PYP_M is independent of the protonation state of the chromophore. It should be noted that the negative band at 1737 cm^{-1} was observed at pH 11.5 (data not shown), indicating that Glu46 is protonated in the dark state even at pH 11.5.

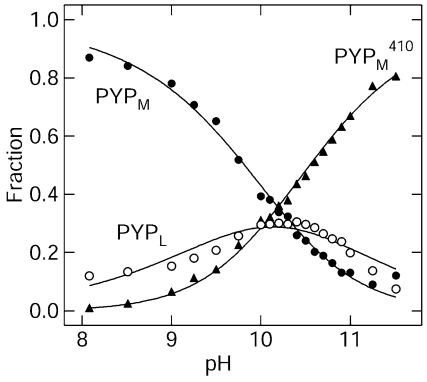

Fig. 5. pH-dependent equilibrium between PYP_M, PYP_M^{410} and PYP_L. Fractions of PYP_M, PYP_M^{410} and PYP_L under >430 nm illumination at various pH values were estimated as shown in Fig. 3. They are plotted against pH.

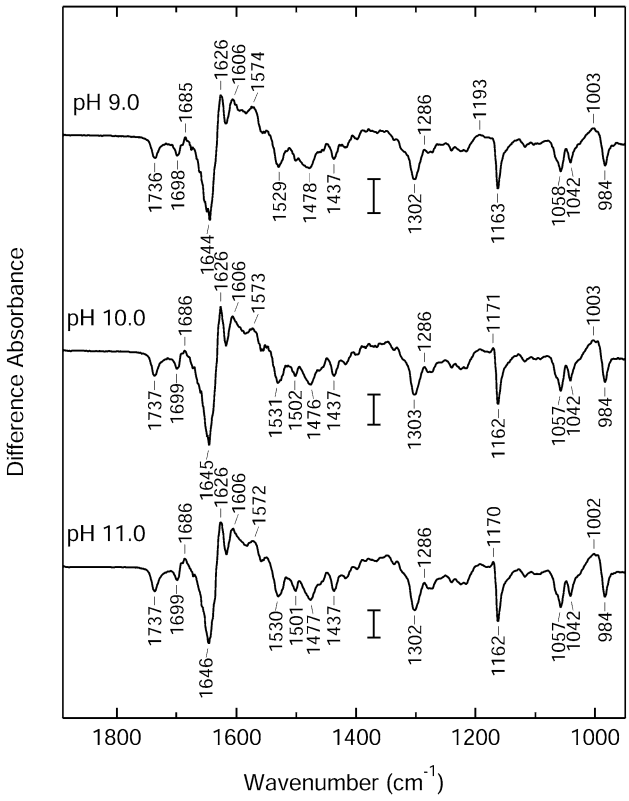

Fig. 6. FTIR spectroscopy of PYP at alkaline pH. PYP was suspended in 100 mM glycine buffer containing 200 mM NaCl at pH 9.0, 10.0, and 11.0. Difference FTIR spectra between dark (negative) and photo-steady-state produced by 436 nm light (positive) were measured at 20 °C. Scale bars represent 0.01 absorbance units. Note that the 1170 cm^{-1} mode observed for photo-steady-state was intensified by alkalization.

The pK_a of the chromophore of PYP_M was 10.2, which is higher than that of denatured *cis-p*-coumaric acid thioester (8.6). In addition, the absorption maximum of PYP_M^{410} (411 nm) was red-shifted from the deprotonated chromophore in the denatured state (399 nm). In the dark state, chromophore is embedded in the hydrophobic pocket and interacts with Tyr42 and Glu46, resulting in an extremely low pK_a of the chromophore and an absorption maximum in the visible region. It is reasonable to speculate that the chromophore of PYP_M interacts with nearby amino acid residue(s), although the interaction may be much weaker than the dark state.

Acknowledgements: This work was supported in part by a Grant-in-Aid for Scientific Research from the Ministry of Education, Culture, Sports, Science and Technology of Japan, and by a grant from Sekisui Integrated Research Inc.

References

[1] Meyer, T.E. (1985) Biochim. Biophys. Acta 806, 175–183.
[2] Borgstahl, G.E.O., Williams, D.R. and Getzoff, E.D. (1995) Biochemistry 34, 6278–6287.
[3] Mihara, K., Hisatomi, O., Imamoto, Y., Kataoka, M. and Tokunaga, F. (1997) J. Biochem. (Tokyo) 121, 876–880.

[4] Genick, U.K., Devanathan, S., Meyer, T.E., Canestrelli, I.L., Williams, E., Cusanovich, M.A., Tollin, G. and Getzoff, E.D. (1997) Biochemistry 36, 8–14.
[5] Imamoto, Y., Koshimizu, H., Mihara, K., Hisatomi, O., Mizukami, T., Tsujimoto, K., Kataoka, M. and Tokunaga, F. (2001) Biochemistry 40, 4679–4685.
[6] Imamoto, Y., Kataoka, M. and Tokunaga, F. (1996) Biochemistry 35, 14047–14053.
[7] Meyer, T.E., Yakali, E., Cusanovich, M.A. and Tollin, G. (1987) Biochemistry 26, 418–423.
[8] Hoff, W.D., van Stokkum, I.H.M., Van Ramesdonk, H.J., van Brederode, M.E., Brouwer, A.M., Fitch, J.C., Meyer, T.E., Van Grondelle, R. and Hellingwerf, K.J. (1994) Biophys. J 67, 1691–1705.
[9] Ujj, L., Devanathan, S., Meyer, T.E., Cusanovich, M.A., Tollin, G. and Atkinson, G.H. (1998) Biophys. J 75, 406–412.
[10] Imamoto, Y., Kataoka, M., Tokunaga, F., Asahi, T. and Masuhara, H. (2001) Biochemistry 40, 6047–6052.
[11] Xie, A., Kelemen, L., Hendriks, J., White, B.J., Hellingwerf, K.J. and Hoff, W.D. (2001) Biochemistry 40, 1510–1517.
[12] Brudler, R., Rammelsberg, R., Woo, T.T., Getzoff, E.D. and Gerwert, K. (2001) Nat. Struct. Biol. 8, 265–270.
[13] Imamoto, Y., Shirahige, Y., Tokunaga, F., Kinoshita, T., Yoshihara, K. and Kataoka, M. (2001) Biochemistry 40, 8997–9004.
[14] Imamoto, Y., Mihara, K., Tokunaga, F. and Kataoka, M. (2001) Biochemistry 40, 14336–14343.
[15] Imamoto, Y., Mihara, K., Hisatomi, O., Kataoka, M., Tokunaga, F., Bojkova, N. and Yoshihara, K. (1997) J. Biol. Chem. 272, 12905–12908.
[16] Imamoto, Y., Kamikubo, H., Harigai, M., Shimizu, N. and Kataoka, M. (2002) Biochemistry 41, 13595–13601.
[17] Ohishi, S., Shimizu, N., Mihara, K., Imamoto, Y. and Kataoka, M. (2001) Biochemistry 40, 2854–2859.
[18] Hendriks, J., van Stokkum, I.H. and Hellingwerf, K.J. (2003) Biophys. J. 84, 1180–1191.
[19] Borucki, B., Otto, H., Joshi, C.P., Gasperi, C., Cusanovich, M.A., Devanathan, S., Tollin, G. and Heyn, M.P. (2003) Biochemistry 42, 8780–8790.
[20] Imamoto, Y., Ito, T., Kataoka, M. and Tokunaga, F. (1995) FEBS Lett. 374, 157–160.
[21] Hendriks, J., Hoff, W.D., Crielaard, W. and Hellingwerf, K.J. (1999) J. Biol. Chem. 274, 17655–17660.
[22] Imamoto, Y., Kataoka, M. and Liu, R.S.H. (2002) Photochem. Photobiol. 76, 584–589.
[23] Meyer, T.E., Devanathan, S., Woo, T., Getzoff, E.D., Tollin, G. and Cusanovich, M.A. (2003) Biochemistry 42, 3319–3325.
[24] Unno, M., Kumauchi, M., Sasaki, J., Tokunaga, F. and Yamauchi, S. (2002) Biochemistry 41, 5668–5674.
[25] Harigai, M., Yasuda, S., Imamoto, Y., Yoshihara, K., Tokunaga, F. and Kataoka, M. (2001) J. Biochem. (Tokyo) 130, 51–56.